3-D convection studies on the thermal state in the lower mantle with post-perovskite phase transition

Masanori Kameyama[1] and David A. Yuen[2]

Received 11 January 2006; revised 3 March 2006; accepted 9 March 2006; published 11 April 2006.

[1] The influences of the post-perovskite (PPV) phase transition on the thermal state in the lower mantle are studied with a three-dimensional model of mantle convection in a Cartesian domain under the extended Boussinesq approximation with variable viscosity and temperature-dependent thermal conductivity. We have varied (i) the intensity of latent heat exchange associated with the PPV transition by increasing the density change and (ii) the temperature at the core-mantle boundary (CMB) which determines the stability field of the PPV phase through the relative positioning with the phase transition temperature at the CMB. We found that the actual PPV transition hardly affects the thermal structure in the lower mantle, although it has a tendency to bend the vertical temperature profile toward the equilibrium thermodynamic conditions of the transition in extreme cases with enhanced latent heat exchange and CMB temperature lower than that of phase transition. **Citation:** Kameyama, M., and D. A. Yuen (2006), 3-D convection studies on the thermal state in the lower mantle with post-perovskite phase transition, *Geophys. Res. Lett.*, *33*, L12S10, doi:10.1029/2006GL025744.

1. Introduction

[2] The experimental discovery of the post-perovskite (PPV) phase by *Murakami et al.* [2004] has greatly stimulated new research directions in many areas in the earth sciences (see *Hirose et al.* [2006a] for a review), such as theoretical mineral physics [e.g., *Tsuchiya et al.*, 2004; *Oganov and Ono*, 2004], seismology [*Hernlund et al.*, 2005], and geodynamics [*Nakagawa and Tackley*, 2004, 2005; *Matyska and Yuen*, 2005, 2006]. Up to now, the geodynamical studies on the PPV transition have been focused on the destabilizing nature of the D″ layer [*Matyska and Yuen*, 2005] and the core-mantle interaction [*Nakagawa and Tackley*, 2004, 2005]. In these studies, the influences of the PPV transition were estimated mainly by varying the Clapeyron slope of the transition. However, there has been scant attention devoted so far to the influences of the variation of other thermodynamic parameters, such as the density change $\Delta\rho/\rho$ associated with the phase transition and the temperature $T_{\rm int}$ of the transition at the pressure of the core-mantle boundary (CMB). Since $\Delta\rho/\rho$ determines the intensity of the latent heat exchange through the thermodynamic Clausius-Clapeyron relation, it is most likely to affect the thermal state near the phase transition regions. On the other hand, the stability field of the PPV phase near the CMB, which is roughly estimated by the relative positioning between the CMB temperature $T_{\rm CMB}$ and the temperature $T_{\rm int}$ of the transition there, is expected to control the positions of the phase transition as well as the number of crossing the phase boundaries [*Hernlund et al.*, 2005]. Moreover, the secular change in $T_{\rm CMB}$ would result in the temporal variation in the PPV stability near the CMB during the Earth's cooling. In this paper we will study the influences on the thermal state in the lower mantle, by a three-dimensional model of mantle convection, with special emphasis to the influence of the variations in $T_{\rm CMB}$ and $\Delta\rho/\rho$.

2. Model Description

[3] A three-dimensional convection in a basally-heated rectangular box of 3000 km height and aspect ratio of $6 \times 6 \times 1$ is considered. We employed an extended Boussinesq approximation [e.g., *Christensen and Yuen*, 1985], where the effects of latent heat, adiabatic heating and viscous dissipation are explicitly included in the energy transport. Temperature is fixed to be $T_{\rm top}$ (=300 K) and $T_{\rm CMB}$ at the top and bottom boundaries, respectively. In this study $T_{\rm CMB}$ is taken to be either 2800 K or 3800 K: The former is lower than the temperature of the PPV transition at the bottom surface (assumed to be 3155 K), while the latter is higher (see below for the meanings). The viscosity η exponentially depends on temperature and depth, with the viscosity variation of $10^{3.5}$ by the temperature change of 2500 K and that of 10^2 with depth. We also take into account a temperature-dependence of thermal diffusivity κ, which mimics the effects of radiative heat transfer [*Hofmeister*, 1999]. Here we assume that κ increases by a factor of 4 with temperature T, as a third-order polynomial of T. Other physical properties, such as thermal expansivity, are kept constant in the entire domain. In all of the calculations we used the Rayleigh number $Ra_{\rm top} = 8 \times 10^6$ and the dissipation number $Di = 0.5$, both defined with the physical properties at the top surface and temperature scale of 2500 K.

[4] In this study we take into account an exothermic phase transition between perovskite to PPV as well as an endothermic transition between spinel and perovskite. Their mechanical and thermodynamical effects are modeled by a phase function Γ [*Christensen and Yuen*, 1985]. In nondimensional forms they are defined by,

$$\Gamma^{(i)} = \frac{1}{2}\left[1 + \tanh\left(\frac{\pi^{(i)}}{\Delta z^{(i)}}\right)\right], \tag{1}$$

$$\pi^{(i)} \equiv -z - \gamma^{(i)}\left(T - T_{\rm int}^{(i)}\right). \tag{2}$$

[1]Earth Simulator Center, Japan Agency for Marine-Earth Science and Technology, Yokohama, Japan.
[2]Department of Geology and Geophysics and Minnesota Supercomputing Institute, University of Minnesota, Minneapolis, Minnesota, USA.

0094-8276/06/2006GL025744$05.00

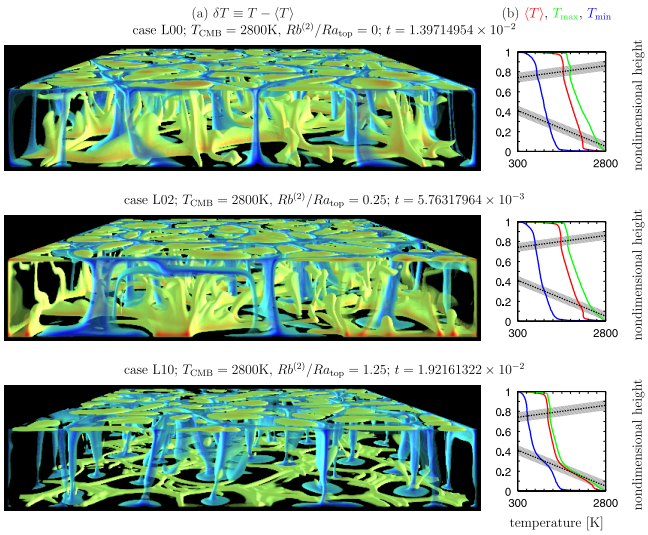

Figure 1. Snapshots of convective flow patterns obtained for the three cases with $T_{CMB} = 2800$ K. (a) The distributions of the lateral thermal anomaly δT. Indicated in blue are the cold anomalies with $\delta T \leq -125$ K, while in yellow to red are the hot anomalies with $\delta T \geq 62.5$ K. (b) Plots against nondimensional height z of the horizontally-averaged $\langle T \rangle$ (red), maximum T_{max} (green) and minimum T_{min} (blue) temperature at the height of z. Also schematically shown in Figure 1b are the phase relations assumed in this calculation. For each phase transition, the hatched regions indicate the regions where $|\pi| \leq \Delta z$, while the thick dotted lines indicate the relations where $\pi = 0$ (or $\Gamma = 0.5$).

Here the index i classifies the phase transitions (1 for spinel-perovskite and 2 for PPV transitions), π is the excess pressure, z is the vertical coordinate pointing upward, γ is the Clapeyron slope, Δz (=0.05) is the depth range for transitions, and T_{int} is the temperature of transition at the bottom surface ($z = 0$). The density change due to phase transition is expressed by another nondimensional parameter called phase boundary Rayleigh number Rb [*Christensen and Yuen*, 1985], whose ratio to Ra_{top} equals the ratio of the density change due to the phase transition and that due to the thermal expansion by a unit temperature change. In this study, the spinel-perovskite transition ($i = 1$) is modeled by a transition at around 660 km depth with $\gamma = -0.12$ and $Rb/Ra_{top} = 1.25$, which correspond to the Clapeyron slope of around -4.3 MPa/K and the density jump of around 10%, respectively. On the other hand, the PPV transition ($i = 2$) is modeled by a transition with $\gamma = 0.36$ and $T_{int} = 3155$ K, while Rb/Ra_{top} is taken to be a free parameter ranging from 0 to 1.25 ($\sim$10% density jump). We note that the above values of adopted parameters are larger than those derived from mineral physics, although there are still uncertainties with these parameters [*Hirose et al.*, 2006b], in order to emphasize the extreme roles played by the PPV transition: The Clapeyron slope (7.5 MPa/K) and the density jump (1.5%) reported by *Tsuchiya et al.* [2004] approximately yield $\gamma^{(2)} = 0.21$ and $Rb^{(2)}/Ra_{top} = 0.19$, respectively.

[5] The computational domain is divided uniformly into $512 \times 512 \times 128$ meshes based on a finite-volume scheme. The calculations are carried out by our newly developed code for the Earth Simulator [*Kameyama et al.*, 2005; *Kameyama*, 2005]. In each run, we continued time-marching calculations until the initial transient behavior disappeared. Each run typically requires 200,000 time steps, and takes about 100 wall-clock hours, using 16 nodes or 128 processors of the Earth Simulator.

3. Results

3.1. Influence of the Density Jump Associated With the PPV Transition

[6] We first present the results of the series L where $T_{CMB} = 2800$ K is kept and, hence, the PPV phase is dominant at the bottom surface (i.e., $T_{CMB} < T_{int}^{(2)}$). In Figure 1 we show for three cases (a) the three-dimensional distributions of lateral thermal anomalies $\delta T \equiv T - \langle T \rangle$, and (b) the plots against height z of the horizontally-averaged $\langle T \rangle$ (red), maximum T_{max} (green) and minimum T_{min} (blue) temperature at height z. The values of T_{max} and T_{min} roughly represent the temperature of ascending and descending flows, respectively. The case L02 is the case with $Rb^{(2)}/Ra_{top} = 0.25$, which is close to the value estimated from mineral physics (see section 2), while the values of $Rb^{(2)}/Ra_{top}$ adopted in cases L00 and L10 are 0 and 1.25, respectively. Namely, in case L00 the PPV transition does not affect the convective nature at all, while in case L10 the effect of density jump associated with the PPV transition is significantly exaggerated.

[7] The plots in Figure 1b show that the temperature profiles have single intersection with each phase boundary (dotted lines in the figure). In other words, the dominant phase monotonously changes from spinel to perovskite and from perovskite to PPV with depth. This also implies that the double-crossing of the PPV transition [*Hernlund et al.*, 2005] never occurs in these calculations. The plots also show that the PPV transition takes place not near the CMB but at a much shallower part. In case L02, for example, the profiles of T_{min}, T_{max} and $\langle T \rangle$ intersect with the PPV phase boundary at $z \sim 0.3$, 0.1 and 0.2, respectively. All of these phenomena come from the low $T_{CMB} < T_{int}^{(2)}$ and resulting low overall temperature.

[8] Figure 1 shows that the thermal state at depth is significantly influenced by a sufficiently large density jump associated with the PPV transition. From a comparison of the three cases we can clearly discern that the thermal state is significantly different in case L10 ($Rb^{(2)}/Ra_{top} = 1.25$), while it is basically the same in case L02 ($Rb^{(2)}/Ra_{top} = 0.25$) with that in case L00. The thermal state in case L10 is characterized by (i) a thick transition region (ranging about $0.1 \leq z \leq 0.3$) between the perovskite to PPV phases and (ii) the vertical profile of $\langle T \rangle$ bent toward the phase equilibrium relations over the depth range. This is due to the steep positive Clapeyron slope as well as the large density jump associated with the PPV transition. Because the Clapeyron slope is steep and positive, the PPV transition is allowed to occur over the broad range of pressure (or depth) according to the temperature variation. In addition, when a significant amount of latent heat is exchanged during the phase transition, the thermal state in the transition region tends to be controlled by the thermodynamic p-T condition, as in the cases with solid-liquid phase transitions in melt dynamics [e.g., *Kameyama et al.*, 1996]. Since the

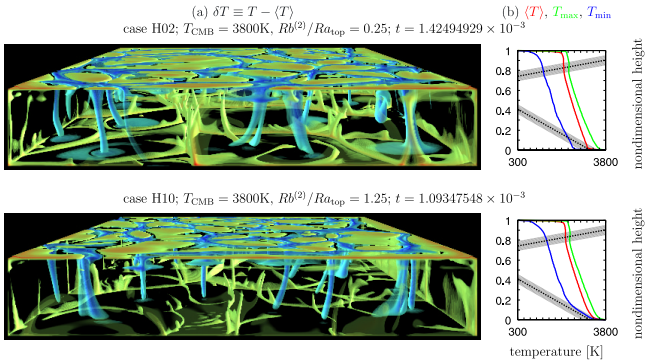

Figure 2. The same as Figure 1 but for the two cases with $T_{CMB} = 3800$ K. Note that the temperature ranges in Figure 2b are different from those in Figure 1b.

rate of latent heat exchange is proportional to the density jump of the phase transition (Rb), a significant amount of latent heat is exchanged in case L10 and, hence, the thermal state in the PPV transition region becomes close to the phase equilibrium condition. We also carried out (though not shown here) calculations by varying $Rb^{(2)}/Ra_{top}$ between 0.5 and 1, and confirmed that the above tendency is more prominent for a larger $Rb^{(2)}$ or, in other words, a higher rate of latent heat exchange.

[9] The snapshot of case L10 also shows other influences of the exaggerated latent heat exchange by a large $Rb^{(2)}$. First is the occurrence of a superadiabatic region in the bottom third of the mantle, which would concur with earlier studies in mineral physics [e.g., *da Silva et al.*, 2000] and seismology [e.g., *Cammarano et al.*, 2005]. This is because the vertical temperature gradient in the PPV transition region becomes close to that of the equilibrium condition of the transition. Second is the "necking" of the surfaces of the cold thermal anomalies at around $z \sim 0.2$, which approximately corresponds to the mean height of the PPV transition (see Figure 1b). As can be seen from the profile of T_{min} in Figure 1b, cold descending flows are heated up at the perovskite to PPV transition because of the latent heat release due to the exothermic transition. This reduces the temperature contrast between the cold descending flows and the surroundings, and hence, results in the "necking" of the cold thermal anomalies. The latter phenomenon is quite similar to "slab detachment" by the exothermic olivine to spinel transition in the upper mantle, suggested by *Brunet et al.* [1998]. This is also consistent with the disappearance of slabs several hundred of kilometers above the D″ layer, inferred by *van der Hilst and Karason* [1999].

3.2. Influence of the Bottom Temperature T_{CMB}

[10] In Figure 2 we present the results of the several cases of the series H where $T_{CMB} = 3800$ K is assumed. In this series, in contrast to the series L, the PPV phase is not dominant at the bottom surface, since $T_{CMB} > T_{int}^{(2)}$. Shown in Figure 2 are the snapshots obtained for the cases H02 and H10 where the values of $Rb^{(2)}/Ra_{top}$ are 0.25 and 1.25, respectively.

[11] The snapshot of case H02 shows that the manner of the PPV transition is quite different from that in case L02. The profile of $\langle T \rangle$ for case H02 shows that the PPV transition takes place on average at around $z \sim 0.05$, much deeper than in case L02 (see also Figure 1b). Moreover, the profile of T_{min} has two intersections with the PPV phase boundary (i.e., double crossing) while that of T_{max} does not at all. This indicates that the PPV phase as well as the double crossing of the phase transition are associated only with the regions near cold descending flows in the lower-most mantle. Figure 2b also shows that the thermal profiles at depth in case H02 are very similar to those expected in cases without the influences of the PPV transition, implying that the influence of the PPV transition with small density jump is rather minor, as also observed in case L02.

[12] From the comparison between the cases H02 ($Rb^{(2)}/Ra_{top} = 0.25$) and H10 (1.25), we can see that the influence of increasing $Rb^{(2)}$ is apparent only near the cold thermal anomalies. Figure 2a shows that in case H10 the cold anomalies are rounded-off above the bottom surface instead of reaching there, while in case H02 they are spread along the bottom surface after having reached there. This is similar to the "necking" of descending flows observed in case L10. Indeed, as can be seen in Figure 2b, the profile of T_{min} in case H10 is bent toward the phase equilibrium relations of the PPV transition. This is also due to the significant latent heat exchange during the PPV transition introduced by the exaggerated $Rb^{(2)}$. In contrast, the profiles of T_{max} are very similar in cases H02 and H10. This reflects the fact that the PPV transition never occurs in the hot anomalies.

[13] The comparison between the series L and H clearly indicates that the influence of increasing $Rb^{(2)}$ on the thermal state becomes smaller for higher T_{CMB}. As can be seen in Figures 1b and 2b, the profiles of $\langle T \rangle$ are raised by increasing $Rb^{(2)}$ only slightly over a rather narrow depth range just above the bottom surface for $T_{CMB} = 3800$ K, while they are significantly affected over a broad depth range for $T_{CMB} = 2800$ K. The difference comes from the difference in the extent of the occurrence of the PPV transition. The profiles of T_{max} and T_{min} show that for high $T_{CMB} > T_{int}^{(2)}$ (series H) the PPV transition takes place only in the cold regions, while for low $T_{CMB} < T_{int}^{(2)}$ (series L) it occurs both in hot and cold regions. Owing to the reduced extent of the PPV transition, the influence on the thermal state is smaller for higher T_{CMB}. In other words, the influence of a higher T_{CMB} is to diminish the tendency toward superadiabaticity. We may expect more superadiabatic situations in a secularly-cooled lower mantle.

4. Concluding Remarks

[14] From a series of calculations with varying $Rb^{(2)}/Ra_{top}$ and T_{CMB} we found that the influence of the PPV transition is prominent only when $Rb^{(2)}/Ra_{top}$ is sufficiently large and T_{CMB} is lower than the temperature of the PPV transition $T_{int}^{(2)}$ at the bottom surface. The former condition requires a sufficient amount of latent heat exchange during the phase transition, while the latter requires that the PPV transition takes place not only in cold but also in hot regions at depth. When the above conditions are met, the vertical temperature profile tends to be bent toward the equilibrium relations of the PPV transition owing to the buffering effect of latent heat exchange. We also found that, for realistic values of the density jump associated with the PPV transition (~1.5%

[*Tsuchiya et al.*, 2004]), the transition is not likely to exert significant influences on the thermal state at depth. However, this result may underestimate the potential influence of the PPV transition, owing to our insufficient treatment of the depth-dependence of physical properties. Indeed, earlier studies based on fully compressible model [*Nakagawa and Tackley*, 2004, 2005] reported that the PPV transition can affect the convective patterns even with a density change of a few percent. In particular, a strong depth-dependence of thermal expansivity, as recently suggested by *Katsura et al.* [2005], may significantly amplify the influence of PPV transition.

[15] During the secular cooling, the nature of ascending plumes would change with time owing to the onset of the PPV transition [*Oganov and Ono*, 2004]. For lower T_{CMB}, these plumes would originate from the CMB with more PPV and, hence, suffer more strongly from the PPV to perovskite transition during their ascent through, for example, the grain size changes. This may imply a significant change in the upward heat transfer from the CMB, as previously estimated by traditional models without the PPV transition [e.g., *Mittelstaedt and Tackley*, 2006].

[16] Our results also demonstrate that, in addition to other thermodynamics, the density change of the phase transition can control the position of the phase transition and, in particular, the number of crossing the PPV phase boundary. In earlier studies [*Hernlund et al.*, 2005; *Nakagawa and Tackley*, 2005], the possibility of "double crossing" of the PPV boundary has been discussed only in terms of the Clapeyron slope and the stability field of the PPV phase near the CMB. However, our results indicate that the above conjecture is valid only when the influence of the latent heat exchange is minor (see Figure 2). We thus conclude that the latent heat energetics is another important agent which may control the nature of phase transitions in the deep mantle.

[17] **Acknowledgments.** We thank two anonymous reviewers for valuable comments. Financial supports from the Stagnant Slab Project, Scientific Research in Priority Areas of Ministry of Education, Culture, Sports, and Technology of Japan (MK), the Math-Geo, CSEDI and ITR programs of the U.S. National Science Foundation (DAY) are greatly acknowledged. All of the calculations presented in this paper were done on the Earth Simulator at Japan Agency for Marine-Earth Science and Technology.

References

Brunet, D., P. Machetel, and D. A. Yuen (1998), Slab weakening by the exothermic olivine-spinel phase change, *Geophys. Res. Lett.*, *25*, 3231–3234.

Cammarano, F., S. Goes, A. Deuss, and D. Giardini (2005), Is a pyrolitic adiabatic mantle compatible with seismic data?, *Earth Planet. Sci. Lett.*, *232*, 227–243.

Christensen, U. R., and D. A. Yuen (1985), Layered convection induced by phase transitions, *J. Geophys. Res.*, *90*, 10,291–10,300.

da Silva, C. R. S., R. M. Wentzcovitch, A. Patel, G. D. Price, and S.-I. Karato (2000), The composition and geotherm of the lower mantle: Constraints from the elasticity of silicate perovskite, *Phys. Earth Planet. Inter.*, *118*, 103–109.

Hernlund, J. W., C. Thomas, and P. J. Tackley (2005), A doubling of the post-perovskite phase boundary and structure of the Earth's lowermost mantle, *Nature*, *434*, 882–886.

Hirose, K., S. Karato, V. F. Cormier, J. P. Brodholt, and D. A. Yuen (2006a), Unsolved problems in the lowermost mantle, *Geophys. Res. Lett.*, *33*, L12S01, doi:10.1029/2006GL025691.

Hirose, K., R. Sinmyo, N. Sata, and Y. Ohishi (2006b), Determination of post-perovskite phase transition boundary in $MgSiO_3$ using Au and MgO internal pressure standards, *Geophys. Res. Lett.*, *33*, L01310, doi:10.1029/2005GL024468.

Hofmeister, A. M. (1999), Mantle values of thermal conductivity and the geotherm from photon lifetimes, *Science*, *283*, 1699–1706.

Kameyama, M. (2005), ACuTEMan: A multigrid-based mantle convection simulation code and its optimization to the Earth Simulator, *J. Earth Simulator*, *4*, 2–10.

Kameyama, M., H. Fujimoto, and M. Ogawa (1996), A thermo-chemical regime in the upper mantle in the early Earth inferred from a numerical model of magma migration in the convecting upper mantle, *Phys. Earth Planet. Inter.*, *94*, 187–216.

Kameyama, M., A. Kageyama, and T. Sato (2005), Multigrid iterative algorithm using pseudo-compressibility for three-dimensional mantle convection with strongly variable viscosity, *J. Comput. Phys.*, *206*, 162–181.

Katsura, T., et al. (2005), Precise determination of thermal expansion coefficient of $MgSiO_3$ perovskite at the top of the lower mantle conditions, paper presented at 3rd Workshop on Earth's Mantle Composition, Structure, and Phase Transitions, Cent. Natl. de la Rech. Sci., Saint Malo, France.

Matyska, C., and D. A. Yuen (2005), The importance of radiative heat transfer on superplumes in the lower mantle with the new post-perovskite phase change, *Earth Planet. Sci. Lett.*, *234*, 71–81.

Matyska, C., and D. A. Yuen (2006), Lower mantle dynamics with the post-perovskite phase change, radiative thermal conductivity, temperature- and depth-dependent viscosity, *Phys. Earth Planet. Inter.*, *154*, 196–207.

Mittelstaedt, E., and P. J. Tackley (2006), Plume heat flow is much lower than CMB heat flow, *Earth Planet. Sci. Lett.*, *241*, 202–210.

Murakami, M., K. Hirose, K. Kawamura, N. Sata, and Y. Ohishi (2004), Post-perovskite phase transition in $MgSiO_3$, *Science*, *304*, 855–858.

Nakagawa, T., and P. J. Tackley (2004), Effects of a perovskite-post perovskite phase change near core-mantle boundary in compressible mantle convection, *Geophys. Res. Lett.*, *31*, L16611, doi:10.1029/2004GL020648.

Nakagawa, T., and P. J. Tackley (2005), The interaction between the post-perovskite phase change and a thermo-chemical boundary layer near the core-mantle boundary, *Earth Planet. Sci. Lett.*, *238*, 204–216.

Oganov, A. R., and S. Ono (2004), Theoretical and experimental evidence for a post-perovskite phase of $MgSiO_3$ in Earth's D'' layer, *Nature*, *430*, 445–448.

Tsuchiya, T., J. Tsuchiya, K. Umemoto, and R. M. Wentzcovitch (2004), Phase transition in $MgSiO_3$ perovskite in the Earth's lower mantle, *Earth Planet. Sci. Lett.*, *224*, 241–248.

van der Hilst, R. D., and H. Karason (1999), Compositional heterogeneity in the bottom 1000 kilometers of Earth's mantle: Toward a hybrid convection model, *Science*, *283*, 1885–1888.

M. Kameyama, Earth Simulator Center, Japan Agency for Marine-Earth Science and Technology, Yokohama 236-0001, Japan. (kameyama@jamstec.go.jp)

D. A. Yuen, Department of Geology and Geophysics, University of Minnesota, Minneapolis, MN 55455–0219, USA. (davey@msi.geo.umn.edu)